Ducted Horizontal Axis Marine Turbine Design for the race of Alderney

Jean-Marc Laurens, M Ait-Mohammed, Mostapha Tarfaoui

Ducted Horizontal Axis Marine Turbine Design for the race of Alderney

J.-M. Laurens, M. Ait-Mohammed, and M. Tarfaoui
Department of Fluid Dynamics, Materials and Structures
ENSTA Bretagne – IRDL, CNRS FRE 3744, France

ABSTRACT: To convert the kinetic energy of marine current into electricity, the most sensible generator is a horizontal axis turbine. The know-how and the tools used for marine propulsion devices find a new range of applications in this field. An academic panel method code developed for the design of bare and ducted marine propellers was applied to design a marine current turbine. The turbine dimension and the tidal current velocity have been taken to fit the conditions in the Race of Alderney. The wing section theory and the optimum rotor theory based on the blade element momentum were used to obtain the design condition and a first geometry approaching the Betz limit for a bare rotor. The panel method was then used to verify the power coefficient obtained in the presence of the 3D effects and if the cavitation constraints are respected. Subsequently, the same panel code was used to verify if the addition of a duct could improve the power output per unit surface. The optimized bare turbine almost reaches 90% of the Betz limit and the optimized duct increases the output by 20% respecting the same overall cross section area.

1 Introduction

This paper takes the text of the previously published article, Laurens et al. (2016) to which have been added new results for the ducted version of the turbine.

Marine renewable energy is a keyword that encompasses many different sources and devices. Exploiting near shore marine currents due to tidal motions is not a new idea. Tidal currents have the great advantage of offering a fully predictable energy source since tidal movements can be determined. The oldest application in France was installed in 1966, Auroy (1967). The geography of the site allowed for the construction of a dam in which 24 reversible 10MWatt turbines are embedded. Although EDF (Electricité De France) is convinced of the worthiness of the Rance power plant, there are some controversial arguments regarding its environmental impact, Charlier (2006). Using today's technology for turbines, the conversion of tidal power into electricity no longer requires large heads hence the dam height can be significantly reduced. Plans for a much larger project of this type in the Channel exist but because of the investment and the environmental impact, it has little chance to be achieved one day. It has also been suggested to divert a part of the flow to harness the tidal power as it has been done for centuries for water mills. Compared to those pharaonic construction projects, the implementation of a water turbine farm appears much more attractive. Although not negligible, the initial investment should be much smaller and above all, its public acceptance is easier since it has no visual impact. To exploit a site without modifying it, certain criteria have to be fulfilled to comply with the economical constraints and the existing technology for marine current systems. If the maximum sinusoidal current speed is less than 1 m/s, the site is not considered and is only deemed attractive if this velocity is more than 1.5 m/s. The water depth also has to be sufficient for a large size water turbine to remain fully submerged at low tide. Using these simple criteria, the European Commission (1996) identified 106 potential sites in Europe and among them 29 have an annual energy content above 10MWh per m^2 of cross-section. The most attractive site in France is the sea passage between Cherbourg in France and the Channel Islands known as Le Raz Blanchard in French and The Race of Alderney in English. The water depth allows for the marine turbine systems to exceed 20 meters of diameter without causing any disruption to maritime traffic and the current velocity peaks above 3 m/s. In order to present some realistic numerical results, the present study is using these data as input.

The survey study performed by Khan et al. (2009) is probably one of the most cited articles because it presents an exhaustive list of existing tidal turbine systems. The most popular design is the axial axis rotor. It has a well-mastered hydrodynamic behaviour since it has propelled planes and ships for more than a century and it is also the most popular design for wind turbines. Compared to vertical axis devices it is simpler and therefore more robust which is an essential quality for a device permanently submerged in an aggressive environment.

The aim of the present study is to apply the know-how and the tools used for the design of marine propellers to the design of horizontal axis water turbines. The preliminary design is obtained using the Blade Element Momentum (BEM) theory. The obtained geometry is then used to generate a surface mesh to solve the potential flow around the rotor using a Boundary Elements Method (also BEM). Unfortunately the two completely different approaches have the same abbreviation. To avoid confusion it is preferable to use the term Panel

Method instead of the Boundary Element Method, at least in this context since most calculations are based on Blade Element Momentum due to the very high aspect ratio of wind turbine. The two methods are explained and applied to the design of a simple bare rotor which reaches 90% of the Betz limit.

Ducted marine propellers are used when the propeller must be heavily loaded as in the case of tugboats and trawlers for example. An accelerating duct reduces the propeller load and thrust, but the duct itself supplies an additional thrust. The total thrust and efficiency is then higher than the one obtained for the rotor alone. In the case of a water turbine, the purpose of a duct will be to supply additional flow to the rotor. It also has to be an accelerating duct which means that the circle carrying the stagnation points must have a larger diameter than the rotor. The panel method is also used to simulate the flow around the ducted rotor. The results tend to indicate that the duct does not significantly increase the power output for a same cross section area.

2 Terminology, theories, models and numerical methods

In marine turbine science, the symbols and the terminology differ from naval propulsion but they can all be translated, however as the purpose is different they are not equally important in both disciplines.

The starting point in water turbine science is the available power, P_a, in Watts in a cross section area A in m^2, crossed by a flow of water. The available power is given by: $P_a = \frac{1}{2}\rho A V_0{}^3$, where ρ is the fluid density (1025 Kg/m^3 for salt water) and V_0 is the flow velocity in m/s. In the targeted application for the Race of Alderney presented in the introduction, a single 20 meter diameter water turbine in the 3 m/s flow therefore has a potential power of 4.35 MWatt. Not all this power can be retrieved by the turbine because it would mean that the flow is fully halted in order to convert all the kinetic energy, and that is obviously not the case. In momentum theory, the water turbine is replaced by a disk with zero thickness. The disk acts as a pressure jump and by applying the Bernoulli equation on each side of the disk, we can obtain the velocity downstream from which the maximum retrievable power is deduced. The ratio of this maximum retrievable power and the available power, called the Betz limit, is equal to 16/27, 59.3%, which means a maximum retrievable power of 2.58 MWatt in our case.

Some authors, Gorban et al. (2001) proposed to refine the actuator disk model used by Betz to obtain a new more restrictive limit. Their new model leads to a new limit of 30.1%, a low percentage which would render most sites, and probably the entire power plant sector, unattractive. Their model is based on Darcy's law which is used for flow through porous media but only applies to Stokes' flows where Reynolds numbers are very low ($R_n < 1$). Bernoulli's equation is used further in the proof but only applies to high Reynolds numbers ($R_n \gg 1$). The strange thing is not that the article has been published but that it has been cited (according to Google scholar) more than 150 times without anyone suspecting a fault. The only author who suspected that something must be wrong was McNaughton (2010) because several experimental results have since demonstrated a higher ratio than the limit of 30.1%.

The performance of marine current energy extractor devices is expressed by the power coefficient, C_p, and its highest value can therefore not exceed 59.3%. When the marine current energy extractor device is a rotor, its delivered power P_D is given as the function of the torque Q and the rotational velocity: $P_D = 2.\pi.n.Q = \omega.Q$, n being the rotational speed in rotations per second. The power coefficient C_p is given by the ratio P_D over P_a. Incidentally, in Bahaj et al. (2006), a mistake has been made in the definition of the C_p which turns this non-dimensional variable into meters. In itself, it is certainly an honest mistake but it has been copied in several other published papers by the same authors and by others.

The non-dimensional frequency which characterizes the working condition of the rotor turbine is the Tip Speed Ratio: $TSR = \frac{\omega R}{V_0}$. The similar coefficient in marine propulsion, Doutreleau et al. (2011), is the advance parameter: $J = \frac{V_0}{n.D}$. The torque and the power delivered to the propeller have the same definition and symbol. The purpose of a marine propeller is to propel the ship and therefore the principal variable is the thrust force, T, given in Newtons. There are two non-dimensional coefficients to characterize the thrust, the thrust coefficient K_T which depends upon n but not upon V_0, and the thrust loading coefficient C_{Th} which depends upon V_0 but not upon n. In turbine nomenclature C_{Th} is C_T and it is a drag coefficient. Similar expressions define the torque coefficients K_Q and C_Q

$$C_{Th} = \frac{T}{\frac{1}{2}\rho A V_0{}^2}, \qquad K_T = \frac{T}{\rho.n^2.D^4},$$
$$C_Q = \frac{Q}{\frac{1}{2}\rho A D V_0{}^2}, \qquad K_Q = \frac{Q}{\rho.n^2.D^5}$$

The efficiency of a propeller, η_0, is defined by the ratio of the power used to thrust the vessel, $P_T = V_0.T$, over the power consumed by the propeller, $P_D = \omega.Q$, thus $\eta_0 = \frac{K_T}{K_Q}.\frac{J}{2\pi}$. Finally, it is convenient to express the turbine power coefficient as a function of K_Q and J, especially when using a propeller computer code to solve the turbine hydrodynamic problem.

$$C_p = \frac{Q\omega}{\frac{1}{2}\rho A V_0{}^3} = \frac{K_q \rho n^2 D^5.\omega}{\frac{1}{2}\rho \frac{\pi D^2}{4} V_0{}^3} = \frac{16 K_q n^3 D^3}{V_0{}^3} = \frac{16 K_q}{J^3}$$

The same momentum theory used to calculate the Betz limit gives a maximum efficiency coefficient for the propeller as a function of the thrust loading coefficient, $\eta_0 < \frac{2}{1+\sqrt{1+C_{Th}}}$.

For a turbine, what remains of the velocity is part of the kinetic energy which cannot be retrieved and for a propeller the acceleration of the flow induced by the propeller is a loss in kinetic energy since it does not contribute to thrust the vessel. Since both limits have the same origin and are derived from the same theory, they should present a direct relationship. We note that, $\frac{C_{Th}}{C_p} = \eta_0$ and since the turbine slows down the downstream flow instead of accelerating it, $\frac{C_t}{C_p} < \frac{2}{1+\sqrt{1-C_T}}$. The maximum value C_p can reach is therefore: $C_T \cdot (1 + \sqrt{1 - C_T})$. In Figure 1 the maximum value C_p can take is plotted against C_T. Not surprisingly we retrieve the Betz limit which occurs when $C_T = {}^8/_9$ as already underlined in Jamieson (2008). Another result of the actuator disk model is that the velocity far behind the rotor is the upstream velocity multiplied by $\sqrt{1 + C_{Th}}$. For a turbine it therefore means that the downstream velocity behind the optimum rotor is 2/3 of the upstream current.
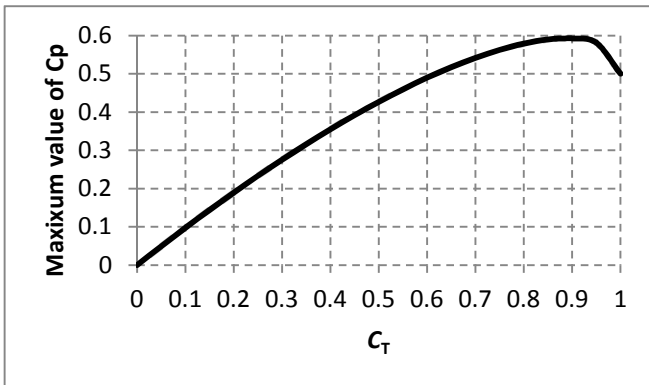

Figure 1. Maximum values C_p can take as a function of C_T.

The most commonly used model for wind turbines is the Blade Element Momentum. It originates from the William Froude's Blade Element Theory which only takes into account the rotation and the axial velocity of the rotor. Momentum theory only describes the axial velocity at the rotor disk and in order to take the rotor induced rotation into account, Prandtl's lifting line theory has to be applied. A brief history of these developments which took place between 1878 and 1930 can be found in Johnson (1980). The blade is discretized into 2D sections, the effective angles of attack are computed from the section pitch, the axial and the tangential velocities as well as the correction for the rotor induced velocities. The hydrodynamic lift and drag coefficients, C_L and C_D, of the 2D sections are given by a 2D simulation using the very popular XFoil software code for instance or by an experimental database such as the Abbott and Von Doenhoff (1959). They depend upon the section geometry and the angle of attack. By

integrating the forces of the sections along the blade span, we obtain the axial and azimuthal forces. The computational method is fast and if the 2D hydrodynamic data take stall into account so will the 3D result. The lifting line theory implies a large aspect ratio which is very legitimate for a wind turbine but is less pertinent for a marine propeller.

To take full account of the 3D effects we use a panel code. The panel methods are based on the potential flow theory. The potential flow model is derived from the incompressible flow Navier-Stokes model. If the flow is assumed irrotational and inviscid, the velocity field derived from a potential function φ, such as $\vec{V} = \vec{\nabla}\varphi$. With these assumptions, the mass conservation equation becomes $\Delta\varphi = 0$ and the momentum equation is reduced to the Bernoulli relation. The Laplace equation for the potential will yield the velocities from which the Bernoulli relation will give the pressure. A slip condition is replacing the Navier-Stokes zero velocity condition at the surface of the objects and for lifting bodies the Kutta condition is imposed at the trailing edge in order to mimic the viscous flow, otherwise the inviscid hypothesis will give zero forces. To solve the system, a very elegant method has been introduced by Hess and Smith (1967), the singularities method. A point singularity respects the Laplace equation everywhere except the point's location where it is not defined. Covering the obstacles by singularities forces the flow to slip on their surfaces. The panel code we use belongs to what Hoeijmakers (1992) refers to as "second generation" panel methods involving the Dirichlet condition (φ=0 in the inner body). Body surfaces are discretized into first order panels carrying constant source and doublet distributions. The wake developing behind the propeller's blades is formed with a sheet of first order panels carrying constant doublet distributions and it is generated over time in a Lagrangian manner. Thanks to the Dirichlet condition imposing the slip condition on the body surface determines the sources directly from the inlet velocity and the normal vectors. Hence, the unknown variables of the problem are the dipoles. The locations of the sheet panel vertices are recalculated at each time step but not the dipoles they carry. Non-lifting bodies such as the hub are discretized using first-order panels carrying constant source and dipole distributions. The propeller hub can be easily modeled this way but in most cases it does not influence the hydrodynamic coefficients, we do not simulate its presence in the results presented here. The code allows for unsteady state flow simulations. The explicit representation of the body thickness leads to an accurate distribution of pressure coefficients (C_p) on the duct and blades surfaces. From the velocities, we compute the local Reynolds number, R_n, on each surface panel which gives us the local friction coefficient C_f using standard formulae: $0.027/\sqrt[7]{R_n}$ for turbulent flow and $0.664/\sqrt{R_n}$ for laminar flow. The transition is forced at $R_n = 5 \times 10^5$. The panel

method only requires a surface mesh of the solid objects. The blades are discretized into 12 sections of 48 panels, the time step is set to correspond to a rotation of 10° and all simulations are run for 72 time steps in order to obtain convergence.

The code can handle lifting and non-lifting bodies and allows for unsteady state flows. It can therefore compute the flow around the rotor even when the inlet velocity is not in the axial direction. A direct simulation of the flow around a ducted rotor is problematic since the rotor blades and the duct are computed as lifting bodies they have to present a sharp trailing edge from which the wake modelled as a sheet of first order panels carrying constant doublet distributions originates. In a single simulation, the panels of the propeller wake sheet will touch and wrongly interfere with the panels of the duct. To avoid numerical errors it has been decided to separate the computation of the flow around the rotor and the computation of the flow around the duct into two different runs. Once the flow around the duct has been solved, we compute the duct induced velocities at the blade control points (i.e. the centres of all panels). The flow around the rotor is then computed in the presence of the duct induced velocities. We then compute the rotor induced velocities on the surface of the duct. The procedure is repeated until convergence which occurs after only a few iterations.

3   Validation

The code has been already verified and validated for many propeller cases and more recently in duct propeller cases, Coache and Laurens (2014). However, since a different field of application is at stake, it is preferable to compare the code with some water turbine experimental results. The experimental results of the three blade turbine rotor described in Bahaj (2007) are used. An automatic mesh generator which has been developed in-house builds the mesh from the chord, pitch, skew, and rake distributions along the blade. These data are given in Bahaj (2007), in this case there is neither skew nor rake. Either a specific profile is given or it is generated from the maximum thickness t/c, the maximum camber distribution f/c and a symmetrical analytic profile. In the experimental report it states that the profile used is a NACA63-8xx where xx is the maximum percentage thickness, i.e. 100.t/c. According to Abbott and Von Doenhoff (1959) the 8 indicates that at its design angle of attack (near 0° and in this case a little above 1°), the profile has a lift coefficient C_L equal to 0.8. The authors do not target any specific design condition but one might suppose that it should close to the highest Cp and before flow separation occurs.
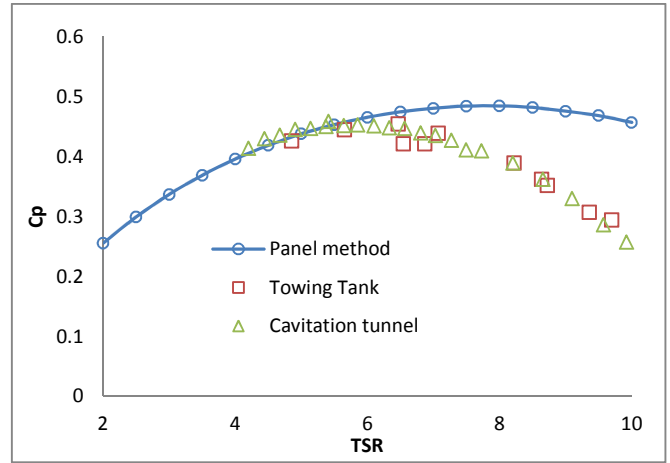

Figure 2. Comparison of power coefficient versus TSR between the potential flow and the experimental results of Bahaj (2007).

The pitch distribution in the experiment can be changed by rotating the blades around their axis. They are named in Bahaj (2007) after the angle of pitch of the tip section. The right part of Figure 2 shows the three blade rotor and the wake sheets developed downstream. The results presented in the left part of Figure 2 are for an angle of pitch at a tip section of 5°. The agreement is good up to TSR=7. The numerical prediction of the hydrodynamic performances in off-design conditions (TSR>7) differs from the experimental results. Baltazar and Falcao de Campos (2009) are using a similar potential flow code and they compared the results of their simulations with those same experimental results. They obtained similar results and proposed a viscous correction using two-dimensional lift and drag data to the take boundary layer flow separation into account, for values of TSR greater than 7. The proposed method permits to get closer to the experimental results. However, there is no reason for a tidal current turbine to operate far beyond its design condition.

4   Design procedure

The design for a propeller is constrained by the thrust it has to provide to the vessel but also by the torque and the RPM given by the engine. Most often the engine is a marine diesel which imposes a severe restriction on the RPM range. Marine current turbine electric generators do not present this restriction, Djebarri et al. (2014). Fixed-pitch blades can be used and torque will be converted into electricity for a very wide range of RPM. Putting aside the structure constraints, the main restrictions are presented by the hydrodynamics. Flow separation and cavitation are to be avoided. The angle of attack and the minimum pressure therefore have to be respected. Starting from a given profile, it must be ensured that its angle of attack does not vary outside the cavitation-free range. It also means that the rotational velocity of the rotor is entirely decided by the profile used on the blade tip. If we use a NACA63-415, this 15% thickness cambered profile best operates when its lift coefficient is equal to 0.4. It then presents a plateau of Cp up to 30% from the leading edge and the recompression starts.

Propellers usually use the NACA66 series because the cavitation is more critical since the vessel will operate in a larger range of conditions. The choice of the NACA63 series yield smaller values for the minimum pressure coefficient Cp but its hydrodynamic coefficients are less subject to vary with the Reynolds number since it should not present any flow separation unless operated well beyond its designed angle of attack. Since the profile is the starting point of the design loop, it is preferable to fully master its geometry. A parametric geometry would be more advantageous. The simplest equation to generate a profile is half the lemniscate of Bernoulli. It generates a profile almost identical to a NACA00 series which has, like the NACA63 series, its maximum thickness at 30% of the leading edge. Furthermore it can be easily cambered by adding a parabolic function of the x-axis to the y coordinate. The geometry is given by:

$$x = \cos(\theta)$$

$$y = \frac{t}{2}\sin(2\theta) + \alpha.x.(x-1)$$

where t is the maximum thickness, θ varies from $\pi/2$ to $3\pi/2$ and α is a camber coefficient. To obtain a profile equivalent to the NACA63-415, α is taken to be -0.08, which corresponds to a maximum camber of f/c=0.02, that is when x=0.5. The top part of Figure 3 presents the two profiles and the distribution of Cp for a 0° angle of attack and a same lift coefficient, $C_L = 0.38$. The minimum value for the Cp is -0.8 in both cases.
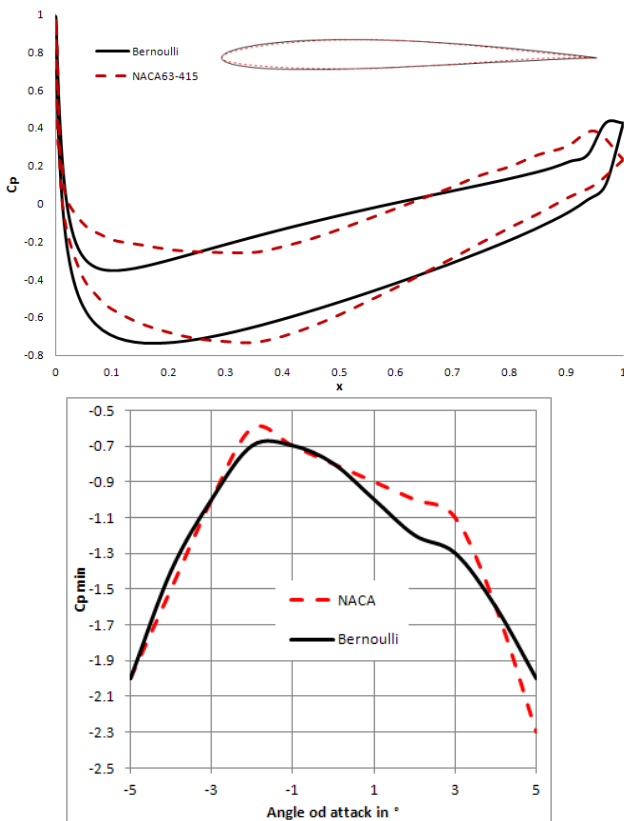

Figure 3. Comparison of the NACA63-415 and the equivalent Bernoulli profile. Top: profiles and Cp curves at 0° angle of attack. Botton: Variation of the Cpmin against the angle of attack.

To verify that both profiles are tolerant to a variation of the angle of attack around its nominal value, Xfoil has been used to obtain the minimum value of the Cp between -5° and 5°. As presented in the bottom part of Figure 3 the curves are very similar and the Cpmin does not drop below -2.5. For this range of the angle of attack, the maximum C_L=1.0 is obtained for 5° and is obviously the same for both profiles. Furthermore, it does not present any flow separation. Exceeding this angle will eventually lead to flow separation and cavitation. The flexibility of the generator should allow us to remain within this range without requiring a variable pitch rotor simply by adjusting the rotational speed.

Once a profile has been chosen, the minimum value of the pressure coefficient Cpmin, taking into account the range of tolerance, is obtained. From this Cpmin value, the maximum velocity at the rotor tip is calculated. To be cavitation free, the minimum pressure computed from the addition of atmospheric, the immersion and the hydrodynamic pressures, $P_{min} = C_{pmin}.0.5.\rho.V^2 + P_{atm} + \rho.g.z$, cannot drop below the saturating vapour pressure, P_v, 2500Pa in cold water. The unknown variable of this relation is the velocity amplitude V, which is the sum of the axial velocity (the current velocity) and the tangential velocity ($\omega.R$). Hence applying the cavitation criterion, the angular velocity is given and therefore, λ, the design TSR. Of course, if for any reason, the obtained angular velocity is not suitable, another profile must be chosen, at least for the blade tip.

As stated in the introduction, the installation in The Race of Alderney allows for 20 meter diameter turbines without causing any perturbation to the maritime traffic and the current velocity peaks above 3 m/s. Using such a profile, the minimum Cp should not drop below -3 and with an immersion of 15 meters, the maximum velocity can safely reach 12 m/s which gives a design TSR, $\lambda = 4$.

The geometrical pitch of the section is computed in order to obtain the design angle of attack (here 0°). The incident velocity is given by the known tangential ($\omega.r$) and axial velocities (V) but they have be corrected due to the action of the rotor on the upstream velocity to become $(1+a').\omega.r$ and $(1-a).V$, respectively. Since the target is to approach the Betz limit, the most logical procedure is to start with the velocity reduction as computed by the momentum theory model. In the procedure of the optimum rotor design theory fully and clearly described in the first chapter of Jamieson (2011), it is rightfully assumed that the Betz limit is reached. In such a case the axial induction, a, is equal to one third and the tangential induction a' varies as $0.5\times(3.\lambda.r/R)^2$. The obtained average pitch P/D using the procedure for our case is then 0.5. The pitch is defined using the conventional propeller pitch definition.

At this stage, only the Blade Element Momentum theory was used to adjust the pitch. The blade element momentum theory produced a first set of values for the pitch distribution. The panel method is then used to assess the hydrodynamic performance taking the 3D effects into account and how far we are from the Betz limit and if we respect the cavitation constraints. The effect of the other geometric characteristics such as the chord spanwise distribution and the number of blades must also be examined.

Although no structural constraints are considered in the present study, common sense is used to determine the ranges of values for the chord and the number of blades. The chord distribution is assumed constant although in a real case it has to be reduced at the tip to avoid tip vortex cavitation.

Table 1 presents the results obtained for the steps of the design procedure. At first the number of blades, Z, is set at 3 and the chord, c/D, is set at 0.1 which corresponds to an aspect ratio AER, close to 0.1. At the design TSR (λ=4), the predicted Cp is 36.1%, which corresponds to 61% of the Betz limit for an output power of 1.57 MWatt. The average pitch is then adjusted and the initial value of 0.5 is changed for 0.4. The AER is then adjusted keeping the number of blades, Z, constant (Z=3) and finally the number of blades is increased keeping the AER constant at its optimum value (0.159). The additional gain obtained when further increasing the number of blades is not significant enough to justify the additional cost involved. The last line of

Table 1 presents a Cp of 52.3%, i.e. 88.2% of the Betz limit for an output power of 2.27 MWatt. This result can be further refined and even automated but the point here is just to show how the numerical tools are used to obtain a design which allows to approach the Betz limit.

Table 1. Cp and output power (in watts) for the different configurations scanned in the optimization process.

Z	P/D	c/D	AER	Kq	Cp	Cp %Betz	Power (watts)
3	0.5	0.1	0.095	0.011	0.361	61	1.6E+06
3	0.4	0.1	0.095	0.013	0.431	73	1.9E+06
3	0.6	0.1	0.095	0.008	0.271	46	1.2E+06
3	0.4	0.07	0.067	0.012	0.395	67	1.7E+06
3	0.4	0.166	0.159	0.013	0.438	74	1.9E+06
3	0.4	0.25	0.239	0.012	0.398	67	1.7E+06
5	0.4	0.1	0.159	0.015	0.492	83	2.1E+06
7	0.4	0.07	0.159	0.016	0.523	88	2.3E+06

It is also ensured at each step that the minimum pressure does not drop below or close to the vaporization pressure. In all the cases the pressure remains above 200,000 Pa.

5 Results

Following the design procedure, a 7 blade water turbine was obtained which should be able to extract half the flow power at its design TSR (λ=4), i.e. 2.27 Mwatt hence more than 7 Kwatt/m^2. Unlike Diesel engines, the generator should adapt its RPM in order to match the design TSR. Nevertheless, some flexibility around the design TSR will still be needed. Figure shows how the Cp varies with the TSR around the design value.
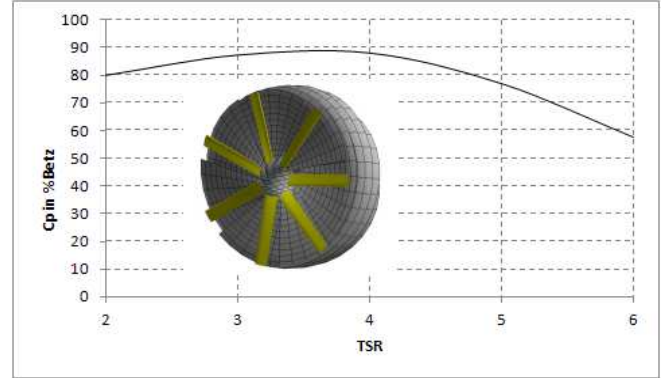

Figure 4. Variation of Cp, given in percent of the Betz limit, around the design TSR

Using the same rotor geometry, it is now examined if the addition of a duct could significantly improve the total output power. An accelerating duct or a diffuser increases the water flow into the rotor and therefore the available power since it is proportional to the cube of the velocity. The duct however uses a significant part of the cross-section area and in order to be of advantage, the power output has to be superior to a bare rotor using the same cross-section area. The relationship is simple; the velocity increase in the rotor, dV, must at least compensate for the loss in diameter, dD in order to maintain the same available power P_A; $(V + dV)^3 . (D - dD)^2 > V^3 . D^2$.

The example presented in Figure 5 shows the results obtained with the potential flow solver for the 7 blades bare rotor of the previous section in comparison to its ducted version. The duct has a total diameter of 20 meters, a NACA0020 section, its length is equal to its radius and the 16 meter rotor is placed at 30% of its leading edge in order to benefit from the maximum velocity. In the left graph of Figure it is shown that if the Cp is computed from the rotor diameter ($Cp = 16 . Kq/J^3$), the Betz limit is exceeded and the results look much higher than for the bare rotor. Now if the Cp is computed using the total cross-section area, Cp*, the results do not favour a ducted turbine. The right graph of Figure , presenting the power output versus rps for a fixed current velocity of 3 m/s, clearly shows that the bare rotor would produce more power than the rotor equipped with the symmetrical duct. The purpose of this example was to show that the power coefficient of a ducted turbine should be computed from the total

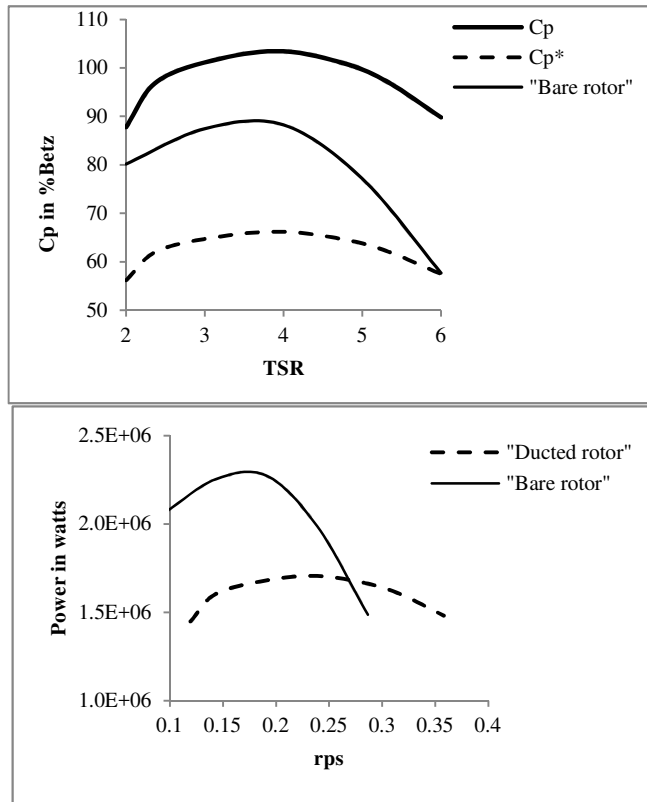area and that the addition of a duct can severely reduce the output power.

Figure 5. Comparison between the rotor in the symmetrical section duct and a bare rotor with a same cross section area. The Cp (top) computed using the rotor diameter gives the advantage to the ducted rotor but using the total area as a reference, Cp*, produces much lower values than the bare rotor. The output power (bottom) as a function of the rotational velocity clearly indicates that the ducted rotor with a same cross section area than the bare rotor will produce far less energy.

The duct has a total diameter of 20 meters, a NACA0020 section, its length is equal to its radius and the 16 meter rotor is placed at 30% of its leading edge in order to benefit from the maximum velocity. In the left graph of Figure it is shown that if the Cp is computed from the rotor diameter ($Cp = 16.Kq/J^3$), the Betz limit is exceeded and the results look much higher than for the bare rotor. Now if the Cp is computed using the total cross-section area, Cp*, the results do not favour a ducted turbine. The right graph of Figure , presenting the power output versus rps for a fixed current velocity of 3 m/s, clearly shows that the bare rotor would produce more power than the rotor equipped with the symmetrical duct. The purpose of this example was to show that the power coefficient of a ducted turbine should be computed from the total area and that the addition of a duct can severely reduce the output power.

To increase the output power the duct must generate enough additional speed to compensate for the loss of rotor diameter. Additional speed can be obtained by choosing a profile for the duct which induces an inward circulation. Since circulation, Γ, and lift, L, are linearly linked by the Joukowski equation ($L =$

$\rho.V.\Gamma$), the profile must present an inward lift. The profile must therefore present a negative angle of attack (diffuser) or a negative camber or a combination of these two. The potential flow code was used to simulate the flow around several configurations. The results in Table 2 are for a duct generated by changing the angle of attack (AoA) of the NACA0020 profile. The ratio of output power over the available power increases with the section AoA, beating the Betz limit after 10° and reaches a maximum at 13° before the loss of diameter takes over.

Table 2. Maximum Cp* and output power (in watts) for the different duct diffuser type configurations.

Angle of attack	Max Cp*	Max output power	Rotor diameter (m)
0°	0.35	1.53E+06	16
3°	0.42	1.84E+06	15.86
6°	0.48	2.11E+06	15.69
9°	0.60	2.52E+06	15.27
11°	0.63	2.73E+06	14.78
13°	0.71	3.08E+06	14.27
15°	0.64	2.79E+06	13.66

A similar table of results was also produced by giving a negative camber to the NACA0020 and a zero degree angle of attack. The results showed that profiles with a same lift coefficient (i.e. a 12% camber with a 0° AoA and a 0% camber with a 5° AoA) produce the same power output which comforts the fact that a same circulation produces a same power output.

The potential flow code cannot predict flow separation and can produce erroneous figures for the section's largest lift coefficients. If we consider the duct as a wing with an infinite span, the flow separation occurrence should coincide with the 2D section. A software code like XFOIL tells us that flow separation occurs at 13% for a cambered profile at 0° AoA and at 13° AoA for the NACA0020 profile. A combination of AoA and camber could generate a higher circulation without flow separation and the length of the duct should also be considered in such a parametric study. Furthermore, a better procedure to predict flow separation in the duct would consist of performing axi-symmetrical RANSE simulations, a technique widely used in propulsion and also used by Hansen et al. (1999) for ducted turbines. In these simulations, the action of the rotor is taken into account as a pressure jump as in the actuator disk model.

6   Conclusion

The know-how and the tools used for marine propulsion devices find a new range of applications in

marine turbines. The theories and the numerical tools used for propeller and ducted propeller design are equivalent. The design procedure presented here shows in a realistic case that the Betz limit can be approached. As for propellers, it cannot be reached because the remaining kinetic energy in the rotor downstream is the principal but not the only cause for efficiency losses. The other causes are the friction on the blade surface, the rotational flow speed induced by the blades, and with a much smaller impact, the tip vortex. Very little can be done about the friction besides keeping the surface smooth. An additional wheel or a stator for instance can be used to retrieve some of the efficiency loss due to the flow rotation and adding some skew is usually the way to reduce the tip vortex intensity.

In marine propulsion, the main device used to retrieve some of the loss due to kinetic energy is an accelerating duct. For a turbine, the accelerating duct will increase the flux in the rotor and will obviously increase the power output when the reference area is the rotor area. To increase the velocity sufficiently in order to compensate for the loss of diameter, the section used to generate the duct has to induce enough circulation. Our simulations predict up to 38% increase of output power for a ducted turbine compared to a bare rotor with the same swept area. It means that we exceed the Betz limit the same way the ducted propeller can exceed the actuator disk theory limit when equipped with a duct. If the addition of a duct can increase the output power, its installation will generate additional cost and technical problems. A quick financial analysis shows that with the current price and increased rate of electricity in France it will take too long to recover the investment in water turbines but the political will of the European Union may change this conclusion. Technically the main problem with the duct will be to resist the non-axial hydrodynamic forces. The material for the rotor will be bronze or stainless steel but the preferred material for the duct so far is composite. It makes it lighter and easier to handle.

References

Laurens, J. M., Ait-Mohammed, M., & Tarfaoui, M. (2016). *Design of bare and ducted axial marine current turbines*. Renewable Energy, 89, 181-187.

Abbott, I. H., & Von Doenhoff, A. E. (1959). *Theory of wing sections: including a summary of airfoil data*. Dover Publications.

Auroy, F. (1967). *L'usine marémotrice de la Rance*. Revue générale de l'électricité, *76*(7-12), 983.

Bahaj, A. S., Molland, A. F., Chaplin, J. R., and Batten, W. M. J. (2007). *Power and thrust measurements of marine current turbines under various hydrodynamic flow conditions in a cavitation tunnel and a towing tank.* Renewable energy, *32*(3), 407-426.

Baltazar J. and Falcao de Campos J.A.C. (2009), *Unsteady analysis of an horizontal axis marine current turbine in yawed inflow conditions with a panel method.,* The 1st International Symposium on Marine Propulsors, SMP'09, Trondheim, Norway, 22-24 June.

Charlier, R. H. (2007). *Forty candles for the Rance River TPP tides provide renewable and sustainable power generation*. Renewable and Sustainable Energy Reviews, 11(9), 2032-2057.

Coache S. & Laurens J.M., (2014), *Toward the optimum design propulsion device for a specific trawler,* 2nd International Conference on Maritime Technology and Engineering, Lisbon, Portugal, October 14-17.

Djebarri S., Charpentier J.F., Scuiller F. and Benbouzid M. (2014), *Systemic Design Methodology for Fixed-Pitch RFPM Generator-Based MCT,* International Conference on Green Energy, Sfax, Tunisia, March 25-27.

Doutreleau, Y., Jodet, L., & Laurens, J. M. (2011). Résistance et propulsion du navire. Edition Ellipse, France.

European Union-Joule II Project (1996), *The exploitation of tidal marine currents* ; Brussels, European Commission, ISSN 1018-5593.

Gorban A., Gorlov A. and Silantyev V. (2001), *Limits of the Turbines Efficiency for Free Fluid Flow,* Journal of Energy Resources Technology. Vol. 123, pp. 311-312.

Hansen M., Sorensen N., Flay R. (1999). *Effect of placing a diffuser around a wind turbine,* European Wind Energy Conference, Nice, France.

Hess, J. L., & Smith, A.M.O. (1967). *Calculation of potential flow about arbitrary bodies*. Progress in Aerospace Sciences, 8, 1-138.

Hoeijmakers, H.W.M. (1992); *Panel Methods for Aerodynamic Analysis and Design*, AGARD Report 783, pp.5.1-5.47.

Jamieson, P. (2011). *Innovation in wind turbine design*, John Wiley & Sons.

Jamieson, P. (2008). *Beating Betz-Energy Extraction Limits in a Uniform Flow Field*. European Wind Energy Conference, European Wind Energy Association Paper CS3. April 2.

Johnson, W. (1980). *Helicopter theory*. Courier Dover Publications.

Khan M.J., Bhuyan G., Iqbal M.T. and Quaicoe J.E. (2009). *Hydrokinetic energy conversion systems and assessment of horizontal and vertical axis turbines for river and tidal applications: A technology status review*, Applied Energy, vol. Vol.86, pp. 1823-1835.

McNaughon J. (2010), *Turbulence Modelling in the Near-Field of an Axial flow Tidal Turbine in Code-Saturne*, First Year ReDAPT project Report, 104 pages.

Thiébot J., Bailly du Bois P., Guillou S. (2015). *Numerical modelling of the effect of tidal stream turbines on the hydrodynamics and the sediment transport – Application to the Alderney Race (Raz Blanchard), France*. Renewable Energy, 75 (2015) 356-365.